

Deficiency of iNOS contributes to *Porphyromonas gingivalis*-induced tissue damage

J. Alayan, S. Ivanovski, E. Gemmell,
P. Ford, S. Hamlet, C. S. Farah

Oral Biology and Pathology, School of
Dentistry, University of Queensland, Brisbane,
Australia

Alayan J, Ivanovski S, Gemmell E, Ford P, Hamlet S, Farah CS. Deficiency of iNOS contributes to *Porphyromonas gingivalis*-induced tissue damage.

Oral Microbiol Immunol 2006: 21: 360–365. © 2006 The Authors. Journal compilation © 2006 Blackwell Munksgaard.

Periodontitis is a chronic inflammatory disease that results in extensive soft and hard tissue destruction of the periodontium. *Porphyromonas gingivalis* possesses an array of virulence factors and has been shown to induce expression of inducible nitric oxide synthase (iNOS) in inflammatory cells. The aim of this study was to investigate the effect of eliminating iNOS in a murine model of *P. gingivalis* infection. This was achieved by utilizing a *P. gingivalis*-induced skin abscess model, and an alveolar bone loss model employing an oral infection of *P. gingivalis* in iNOS knockout mice. The results indicated that iNOS knockout mice exhibit more extensive soft tissue damage and alveolar bone loss in response to *P. gingivalis* infection compared to wild-type mice. The local immune response to *P. gingivalis* in iNOS knockout mice was characterized by increased numbers of polymorphonuclear monocytes, while the systemic immune response was characterized by high levels of interleukin-12. The iNOS is required for an appropriate response to *P. gingivalis* infection.

Key words: alveolar bone loss; inducible nitric oxide synthase; knockout mice; *Porphyromonas gingivalis*

Camile S. Farah, Senior Lecturer in Oral Medicine & Pathology, School of Dentistry, The University of Queensland, Brisbane, Qld 4072, Australia
Tel.: +61 7 3365 8840;
fax: +61 7 3365 1109;
e-mail: c.farah@uq.edu.au

Accepted for publication April 24, 2006

Nitric oxide (NO) is a short-lived free radical involved in the regulation of diverse physiological and pathological mechanisms (5, 23). The biosynthesis of NO occurs through the catalysis of L-arginine by the family of isoenzymes that are globally known as NO synthases (NOS). Currently, at least three distinct isoforms of NOS have been isolated and cloned: endothelial NOS (eNOS or NOS-1), inducible NOS (iNOS or NOS-2) and neuronal NOS (nNOS or NOS-3). Constantly present in resting cells, eNOS and nNOS produce NO in low concentrations leading to numerous effects including smooth muscle relaxation and inhibition of platelet aggregation and adhesion (9). In contrast, iNOS is induced in macrophages and polymorphonuclear cells only after its stimulation by inflammatory mediators such as interleukin-1 (IL-1), tumour nec-

rosis factor (TNF), interferon- γ (IFN- γ) and lipopolysaccharide (LPS) (4). This inducible process yields high amounts of NO for long periods of time (19).

Periodontitis is a chronic inflammatory disease that results in extensive soft and hard tissue destruction of the periodontium. The extent of disease is largely based on the host's inflammatory response to bacteria that are present in plaque. Indeed, the pathogenesis of periodontitis is complex, with a systemic response also accompanying the local destruction. *Porphyromonas gingivalis* is a gram-negative, black-pigmented anaerobic bacterium which has been shown to be a major pathogen in periodontitis (28). It possesses an array of virulence factors and has been shown to induce iNOS expression in inflammatory cells (18). Since NO is thought to play an important role in host

defence against bacterially induced tissue destruction (14), the role of iNOS in the response to the systemic and local effects of bacterial infection is of considerable importance in understanding the pathogenic mechanisms involved in periodontitis.

One of the main manifestations of periodontitis is bone loss, which compromises the attachment apparatus of the tooth and may lead to tooth loss. Osteoblasts and osteoclasts both produce and respond to NO (6, 25). Studies *in vitro* have shown a biphasic effect of NO on both osteoblastic and osteoclastic activity. Low levels of NO promote osteoblastic growth and differentiation in both an autocrine (26) and a paracrine fashion (6, 7). Conversely, high levels of NO have been shown to inhibit both osteoblastic and osteoclastic growth and differentiation (6, 20, 24, 25, 32).

The effects of NO on bone metabolism remain ambiguous with studies reporting both stimulatory and inhibitory effects, depending on the levels of NO and the model used (8, 24). In addition, experimental data on the contribution of iNOS to the host's defence against a specific periodontal pathogen remains scarce. As such, the aim of this study was to investigate the local and systemic consequences of eliminating iNOS in a murine model of *P. gingivalis* infection. This was achieved by utilizing a *P. gingivalis*-induced skin abscess model to monitor the acute reaction, and an alveolar bone loss model employing an oral infection of *P. gingivalis* in iNOS knockout mice to measure changes to alveolar bone over time.

Materials and methods

Mice

Specific pathogen-free female knockout mice C57BL/6J \times 129iNOS^{-/-}, and their respective wild-type controls C57BL/6J \times 129iNOS^{+/+}, 6–8 weeks of age, were obtained from the Animal Services Division, Australian National University, Canberra, and bred at the Herston Medical Research Centre, with the genotypes checked regularly by polymerase chain reaction. Animal experiments were approved by the Animal Experimentation Ethics Committee of the University of Queensland, and carried out in accordance with the National Health and Medical Research Council's Australian Code of Practice for the Care and Use of Animals for Scientific Purposes, 1997. Mice were housed in filter-top cages in a PC2 facility, and provided with food and water *ad libitum*. All experiments were repeated twice.

Bacteria

P. gingivalis W50 was used in this study. The bacterium was cultured anaerobically as described previously (3). Briefly, the bacterium was cultured on Wilkens Chalgrens agar plates (Oxoid, Adelaide, South Australia) prepared from Wilken Chalgrens broth (Oxoid; 33 g/l) with the addition of agar (10 g/l) and 5% laked sheep blood. The plates were incubated for 4 days at 37°C in an atmosphere of 10% H₂, 10% CO₂ and 80% N₂ in an anaerobic cabinet (Katec Pty Ltd, Adelaide, South Australia). The black-pigmented colonies from plates were subcultured into Wilkens Chalgrens broth and incubated as above. Purity was monitored by Gram stain and by subculture to Wilkens Chalgrens agar

plates. Bacterial numbers in the broth cultures were determined by counting in a Helber bacterial counting chamber under phase-contrast microscopy. The bacteria were harvested from 48-h broth cultures. The bacteria were suspended in reduced phosphate-buffered saline (PBS) at the appropriate concentration for injection (10¹⁰/ml) and transported in an anaerobic state for injection. All inoculation and sampling procedures were conducted under halothane anaesthesia (Veterinary Companies of Australia, Artarmon, NSW, Australia) using an inhalation apparatus (Fluortec, Mediquip, Brisbane, Qld, Australia) and a scavenging system (Omnicon Fresh Air Cannister, Bickford Inc., NY).

Skin challenge

Mice were injected subcutaneously at two sites on the dorsal surface, approximately 1 cm on either side of the midline, as described previously (13). Mice were injected with 100 μ l/site of 10¹⁰/ml *P. gingivalis*, or the equivalent volume of sterile PBS. Lesion size and number were monitored for a 10-day period. Ten days after challenge, mice were anaesthetized, blood samples were collected by direct heart puncture and then the mice were sacrificed. Serum from mice in each group was pooled, and clarified (10,000 g for 15 min) for the determination of cytokine and antibody levels. Spleens were removed, worked through cell strainers (Falcon, Becton Dickinson, Franklin Lakes, NJ) and the resulting suspensions were washed and centrifuged on Ficoll-Paque gradients to obtain mononuclear cell suspensions. T cells were then stained for intracytoplasmic cytokines and analysed by two-colour flow cytometry as described below.

Flow cytometric analysis

The per cent of CD4 and CD8 T cells extracted from spleens at day 0 and day 10 following challenge were stained for intracytoplasmic IL-4, IL-10 and IFN- γ as described previously (12, 13). Briefly, surface membrane staining of CD4 and CD8 cells was achieved using fluorescein isothiocyanate-conjugated rat anti-mouse CD4 or CD8 (PharMingen, San Diego, CA), followed by fixation of these cells in paraformaldehyde, permeabilization using Proteinase K and then incubation with phycoerythrin-conjugated rat anti-mouse IL-4, IL-10 or IFN- γ (PharMingen). For the assessment of non-specific binding of the rat antibodies to the mouse cell surface

antigens, phycoerythrin- and fluorescein isothiocyanate-conjugated specific rat immunoglobulin isotypes (PharMingen) were used in place of the CD4 or CD8 antibodies and the anti-cytokine antibodies. Dual-colour flow cytometry on a FACSCalibur (Becton Dickinson, Mountain View, CA) was used to analyse 10,000 stained cells from each sample and the percentages of CD4 and CD8 cells which were positive for IL-4, IL-10 and IFN- γ were determined.

Detection of serum cytokines following skin challenge

Serum from *P. gingivalis*-challenged and PBS control groups was assayed for IL-4, IL-10, IL-12, IFN- γ and TNF by enzyme-linked immunosorbent assay using Opt-EIA Mouse Cytokine Sets (PharMingen) according to the manufacturer's instructions. Briefly, immuno-polysorb microtitre plates (Nunc, Roskilde, Denmark) were coated with capture antibody. After blocking non-specific sites, diluted serum samples were added, followed by biotinylated anti-mouse monoclonal antibody and avidin-horseradish peroxidase conjugate. The substrate containing tetramethylbenzidine and hydrogen peroxide was then added for colour development. The reaction was stopped after 30 min with 1 mol H₃PO₄. The optical density of the wells was read in a Bio-Rad microplate reader (Bio-Rad Laboratories, Regents Park, NSW, Australia) at 450 and 570 nm. Cytokine concentrations in the serum samples were determined from a standard curve of dilutions of a known standard. Negative control wells used PBS in place of the serum samples to determine background values.

Detection of anti-*P. gingivalis* antibodies following skin challenge

Pathogen-specific immunoglobulins were quantified using an enzyme-linked immunosorbent assay. Microtitre plate wells (Nunc, Maxisorp) were coated with *P. gingivalis* (1 μ g/ml). After blocking with 1% bovine serum albumin, diluted serum samples were added followed by goat anti-mouse immunoglobulin G1 (IgG1), IgG2a- or IgM-specific horseradish peroxidase-labelled monoclonal antibody (Caltag Laboratories, Burlingame, CA). The substrate containing 0.0075% H₂O₂ and 2.5 mmol *o*-toluidine (Eastman Kodak, Rochester, NY) was then added and the colour reaction was stopped after 10 min with 1 mol HCl. The optical

density of the wells was read in a Bio-Rad microplate reader, at 450 and 655 nm. Antibody concentrations in the serum samples were determined from a standard curve of known concentrations of purified mouse IgG1, IgG2a or IgM (Caltag Laboratories) that was coated onto each plate. Negative control wells were prepared by adding carbonate buffer only to the wells.

Histopathology

Skin lesions removed from mice sacrificed on day 1 and day 10 following challenge were fixed in 10% neutral buffered formalin (pH 7.0), embedded in wax, sectioned and stained with haematoxylin and eosin for examination by light microscopy.

Oral infection

The *P. gingivalis* infection was established in the gingival tissues according to the method of Baker et al. (1). Mice were given sulfamethoxazole–trimethoprim (Bactrim) *ad libitum* in de-ionized water for 10 days before infection, followed by a 4-day antibiotic-free period. Mice were inoculated orally with 10^{10} colony-forming units of live *P. gingivalis* in 100 μ l PBS by gavage three times at 2-day intervals for 1 week. Controls included sham-infected mice, which received the antibiotic water pre-treatment, and the PBS gavage without *P. gingivalis*. Ten weeks after the last gavage, mice were sacrificed and samples were collected. A separate group of iNOS^{+/+} and iNOS^{-/-} mice received no experimental procedures but were sacrificed at 6, 16 and 30 weeks of age.

Histomorphometric bone analysis

After the animals were sacrificed, their skulls were dissected and jaws were defleshed after treatment in 6% Triton-100 at 85°C for 3 h. Subsequently, the samples were immersed overnight in 3% H₂O₂, followed by 20-s wash with 1% NaOCl, air-dried and stained with 0.5% eosin for 5 min followed by 1% methylene blue for 1 min to delineate the cemento-enamel junction (CEJ) more clearly.

Alveolar bone loss was measured morphometrically according to the method of Tatakis and Guglielmoni with minor modifications (30). The area of bone loss (mm²) was calculated as the sum of the exposed molar root surface on all three molars, in both the maxilla (buccal and palatal) and mandible (lingual). Blinded measurements were performed using a dissecting microscope and a computer-

assisted image analysis system (Axiovision; Carl Zeiss Vision, Oberkochen, Germany) by a sole blinded operator. The area of interest was highlighted by accurately circumscribing the area bounded by the CEJ and alveolar bone crest. These represent both the occlusal and apical boundaries of each molar respectively. The mesial and distal boundaries were represented by the mesial and distal line angles of each molar respectively. A scale was obtained using a 1- μ m microscopic slide, mounted at the same magnification as the jaw specimens. Intra-observer reproducibility was determined to be approximately 98%.

Statistics

Quantitative data were analysed using the statistical features of GRAPHPAD PRISM Version 2.01 (GraphPad Inc., San Diego, CA). Student's *t*-test and one way analysis of variance were used with $P < 0.05$ unless otherwise indicated.

Results

Lesion dimensions

P. gingivalis-infected iNOS^{-/-} mice exhibited a significantly larger lesion diameter at day 1 when compared to iNOS^{+/+} mice ($P < 0.01$). This was significantly reduced by day 10 to dimensions similar to those seen in the iNOS^{+/+} mice (Fig. 1). There was no significant difference in lesion diameter in the infected iNOS^{+/+} mice between days 1 and day 10. No lesions were detectable in the sham-infected

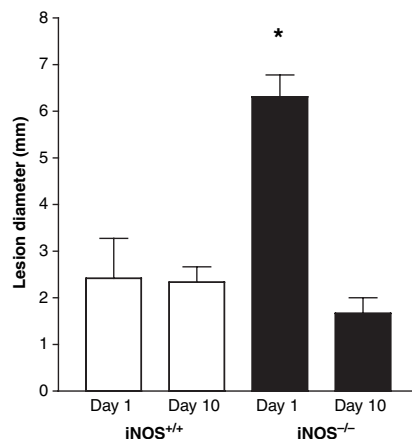


Fig. 1. Diameter of skin lesions of both iNOS^{-/-} and iNOS^{+/+} mice at day 1 and day 10 following *P. gingivalis* challenge. Data points represent the mean \pm SEM for a minimum of seven mice/group. *Significant difference between iNOS^{-/-} and iNOS^{+/+} mice on day 1 ($P < 0.01$).

iNOS^{-/-} or iNOS^{+/+} mice at day 1 or day 10.

Histopathology of skin lesions

An extensive polymorphonuclear cell (PMN) infiltrate was seen in iNOS^{-/-} mice (Fig. 2A), while a more diffuse pattern was observed in iNOS^{+/+} mice at day 1 following *P. gingivalis* challenge (Fig. 2B). The iNOS^{-/-} mice also displayed large, dense, well-organized granulomas on day 10 (Fig. 2C), mostly composed of PMNs (Fig. 2D).

Splenic cytokine profiles

A greater percentage of IL-4-, IL-10- and IFN- γ -positive CD4 T cells was detected in the iNOS^{+/+} mice compared to iNOS^{-/-} mice, 10 days after skin challenge with *P. gingivalis* (Fig. 3A). A similar pattern was observed in CD8 T cells, except for IL-4-positive CD8 cells (Fig. 3B).

Serum cytokine profile

Moderate amounts of IL-12 (171.5 pg/ml) and lower amounts of IL-10 (65.17 pg/ml) were detected in the *P. gingivalis*-infected iNOS^{-/-} mice, while both cytokines were absent in *P. gingivalis*-infected iNOS^{+/+} mice. IL-4, IL-10 and TNF were not detected above baseline in either of the mouse strains challenged with *P. gingivalis*. No cytokines were detected in sham-infected control mice, regardless of the mouse strain.

Serum anti-*P. gingivalis* antibody levels

Moderate levels of IgG1 were noted in both iNOS^{+/+} and iNOS^{-/-} mice following skin challenge with *P. gingivalis* compared to sham-infected mice (Table 1). The level of IgG1 was slightly higher in the *P. gingivalis*-infected iNOS^{-/-} mice compared to *P. gingivalis*-infected wild-type mice. Minimal levels of IgG2a were detected in *P. gingivalis*-challenged mice compared to sham-infected mice in both strains of mice, with higher levels again observed in *P. gingivalis*-infected iNOS^{-/-} compared to *P. gingivalis*-infected wild-type mice. No IgM was detected in any of the groups.

Alveolar bone loss

There was significantly more naturally occurring bone loss ($P < 0.05$) seen at 30 weeks of age compared to 6 and 16 weeks in both iNOS^{+/+} and iNOS^{-/-} mouse groups (Fig. 4), but there was no

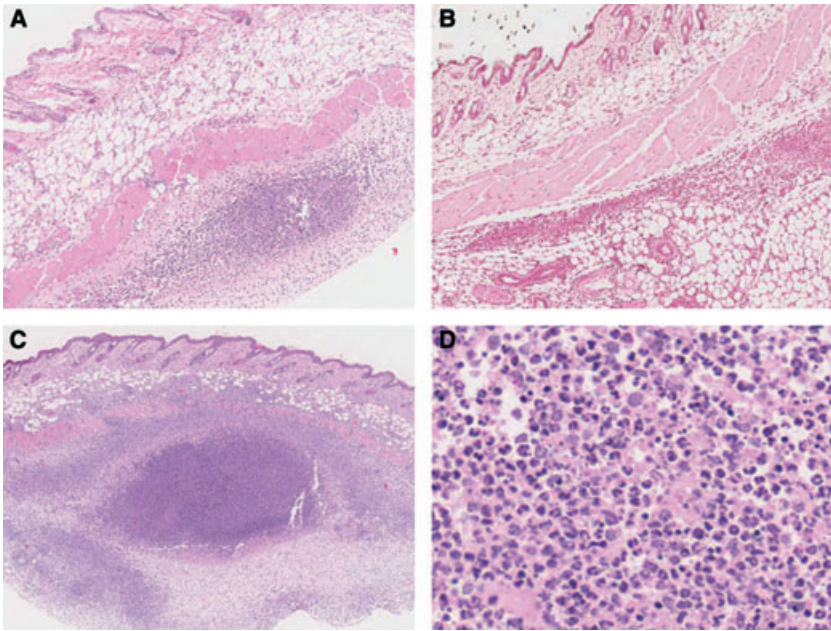


Fig. 2. An extensive PMN infiltrate can be seen in iNOS^{-/-} mice at day 1 following *P. gingivalis* challenge (A; ×4) compared to iNOS^{+/+} mice (B; ×4). Well-organized granulomas seen in iNOS^{-/-} mice on day 10 (C; ×4) were mostly composed of PMNs (D; ×40). All sections stained with haematoxylin & eosin.

A significantly greater amount of alveolar bone loss ($P < 0.0001$) occurred in the *P. gingivalis*-infected iNOS^{-/-} mice compared to the infected iNOS^{+/+} mice 10 weeks after oral inoculation (Fig. 5). There was more than a two-fold increase in alveolar bone loss in the *P. gingivalis*-infected iNOS^{-/-} mice compared to the *P. gingivalis*-infected iNOS^{+/+} mice, as is clearly demonstrated in Fig. 6. There was also a significant increase in alveolar bone loss ($P < 0.0001$) between infected and uninfected iNOS^{-/-} mice (Fig. 5).

Discussion

NO is thought to play an important role in host defence against bacterially induced tissue destruction (14). Various models of iNOS knockout animals have shown an increased susceptibility to infections with a variety of pathogens (21, 34). In this study, both the local and systemic effects of iNOS gene deletion were studied in a mouse model utilizing infection with *P. gingivalis*, a major pathogen in periodontitis.

The increased skin lesion diameter seen in the *P. gingivalis*-infected iNOS^{-/-} mice supports the concept that at the local level iNOS is an important host factor that provides protection against bacterially induced soft tissue destruction, and suggests that iNOS-derived NO has a protective role against this micro-organism. This conclusion is supported by Gyurko et al.

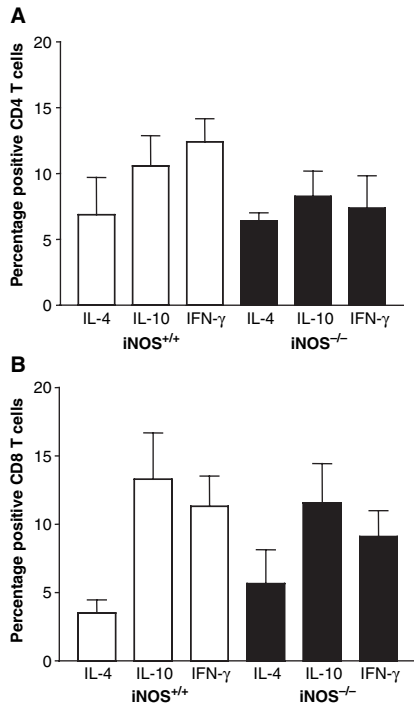


Fig. 3. Percentage of IL-4-, IL-10- and IFN-γ-positive splenic CD4 (A) and CD8 (B) T cells in both iNOS^{+/+} and iNOS^{-/-} mice at day 10 after *P. gingivalis* skin challenge. Data points represent the mean ± SEM for a minimum of five mice/group. No significant difference was noted between the mouse groups.

significant difference in alveolar bone loss between these two groups of mice at each of these specific time-points.

Table 1. Serum anti-*P. gingivalis* IgG1 and IgG2a levels at day 10 after skin challenge

	IgG1 (μg/ml)	IgG2a (μg/ml)
iNOS ^{+/+} PBS	0.0	0.0
iNOS ^{+/+} Pg	79.8	1.2
iNOS ^{-/-} PBS	2.6	0.6
iNOS ^{-/-} Pg	99.0	15.9

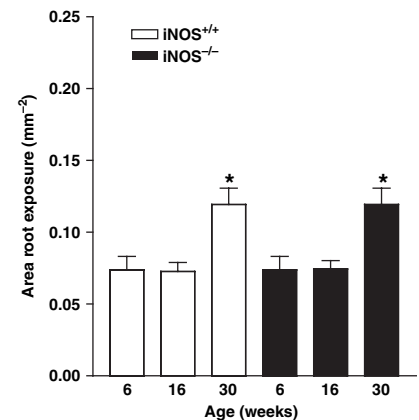


Fig. 4. Area of alveolar bone loss (mm²) in naturally-aged iNOS^{+/+} and iNOS^{-/-} mice at 30 weeks of age compared to mice aged 6 and 16 weeks. Data points represent the mean ± SEM for a minimum of three mice/group. *Significantly more alveolar bone loss occurred in the 30-week-old mice compared to the 6- and 16-week-old mice in each mouse strain ($P < 0.05$). There was no significant difference between the mouse strains at any of the time-points.

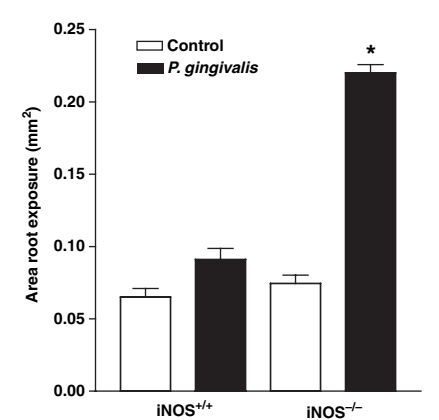


Fig. 5. Area of alveolar bone loss (mm²) in *P. gingivalis*-induced iNOS^{+/+} and iNOS^{-/-} mice at 10 weeks after oral challenge compared to uninfected control mice. Data points represent the mean ± SEM for a minimum of five mice/group. *Significantly more alveolar bone loss in infected iNOS^{-/-} mice compared to infected iNOS^{+/+} and uninfected iNOS^{-/-} control mice ($P < 0.0001$). There was no significant difference between infected and uninfected iNOS^{+/+} mice.

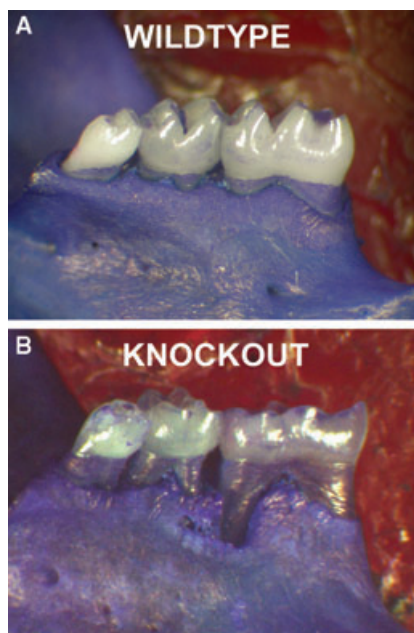


Fig. 6. Mandibular lingual aspect of representative bone loss in *P. gingivalis*-infected $iNOS^{+/+}$ (A) and $iNOS^{-/-}$ (B) mice at 10 weeks after oral challenge. The greater area of bone loss in $iNOS^{-/-}$ mice is clearly evident compared to $iNOS^{+/+}$ mice. There is more exposed root surface and furcation involvement in the $iNOS^{-/-}$ mice.

(14), who reported similar findings in $iNOS$ knockout mice after subcutaneous chamber inoculation with *P. gingivalis*.

Histological analysis of the soft tissue lesions indicates that PMN numbers were affected by the $iNOS$ status of the mouse. In the absence of $iNOS$ in the knockout mice there was an increase in the number of PMNs seen soon after *P. gingivalis* challenge, contributing to an increased lesion size. In contrast, the presence of induced NO in the wild-type animals resulted in a more diffuse PMN infiltrate, suggesting once again that $iNOS$ -derived NO is protective.

Traditionally in mice, the macrophage has been thought to be the major source of NO (35), however recent evidence suggests that PMNs are also an important source of NO in human periodontitis (2), and in *P. gingivalis*-induced skin lesions (14). There is also evidence that endogenously released NO can be cytoprotective and that the impact of $iNOS$ on PMN viability occurs on both a molecular and a cellular level (14, 31). These findings are important in the context of periodontal disease, where PMNs are part of the first-line defence against a bacterial infection and play a protective role (11). Indeed, PMN disorders, such as cyclic neutropenia

(10), Chediak–Higashi syndrome (16) and leukocyte adhesion deficiency syndrome (29), result in extensive periodontal breakdown and tooth loss at an early age. NO derived from PMNs in diseased periodontal tissues may contribute to their protective effect.

Systemically, elevated levels of IL-12 were detected in the serum of *P. gingivalis*-infected $iNOS$ knockout mice following skin challenge. Studies have shown that NO has a regulatory role in the immune system by inhibiting T helper type 1 (Th1) cell development (17, 22). NO mediates this inhibition by selectively down-regulating IL-12 synthesis (17), which is a potent inducer of Th1 differentiation, thereby blocking the amplification circuit created with macrophages and IFN- γ . Our results also showed that the Th1 response mediated by IL-12 in the serum was somewhat counterbalanced by a Th2 response determined by increased amounts of IL-10, and elevated levels of IgG1 compared to IgG2a. Furthermore, there were no significant differences between $iNOS$ knockout mice and wild-type mice with respect to splenic intracellular cytokine expression (IL-4, IL-10 and IFN- γ). These data suggest that the status of $iNOS$ has no significant impact on polarizing the immunological response towards either Th1 or Th2. These results are in agreement with the serological findings of another study utilizing $iNOS$ knockout mice (14).

The effect of $iNOS$ on bone is controversial and complex. Studies examining the role of NO on bone cell activity have reported both stimulatory and inhibitory effects on bone remodelling, depending on the level of NO and the model used (8, 24). Expression of $iNOS$ can be induced in bone by bacterial LPS and pro-inflammatory cytokines (33), with osteoblasts being the main source of $iNOS$ (6). This leads to high expression of NO and inhibition of bone resorption (6, 20, 24, 32).

It is well known that LPS stimulates the release of pro-inflammatory cytokines such as IL-1 and TNF to induce osteoclast proliferation and differentiation (27). These cytokines also stimulate osteoblasts to release osteolytic mediators that promote bone resorption. The high concentration of NO has been shown to be responsible for the inhibitory effect of IFN- γ on bone resorption that is stimulated by IL-1 and TNF. This is thought to be a result of the inhibition of osteoclast formation, activity and induced apoptosis of osteoclast progenitors (32).

The lack of alveolar bone resorption seen in the infected wild-type animals is

likely to be because of high concentrations of NO being produced after $iNOS$ induction by *P. gingivalis* LPS, and its inhibitory effects on osteoclasts. The results of our study support the concept that $iNOS$ protects against *P. gingivalis*-induced alveolar bone resorption, and hence its absence in the $iNOS$ knockout mice potentiates *P. gingivalis*-induced bone resorption. Naturally occurring alveolar bone loss was found to be unaffected by the presence or absence of $iNOS$, but this was dependent on the age of the mice. The protective properties of NO are obviously highlighted when induced by inflammatory stimuli such as LPS. In the absence of an inflammatory stimulus, the presence or absence of $iNOS$ does not seem critical in maintaining bone turnover.

These findings are in contrast to a recent study by Gyurko et al. (15) who showed that *P. gingivalis*-infected $iNOS$ knockout mice showed no increase in alveolar bone loss, whereas $iNOS$ wild-type mice did (15). Moreover, they showed that $iNOS$ knockout mice displayed more alveolar bone loss in the absence of bacterial challenge compared to wild-type mice from the age of 6 weeks onwards. These apparently conflicting data may be partially explained by variations in the experimental design. Gyurko et al. observed *P. gingivalis*-induced bone loss at 6 weeks after challenge whereas in the current study our measurements were taken at 10 weeks after infection. We did not note any changes in alveolar bone loss at 6 weeks post challenge (data not shown). Differences in the relative pathogenicity of the *P. gingivalis* strains used in these studies may have also contributed to these discrepancies. In addition, Gyurko et al. used C57BL/6 mice as wild-type controls, whereas the wild-type control mice in our study are on the C57BL/6 \times 129 background. Furthermore, we measured the area of alveolar bone loss on three molar teeth in both the mandible and maxilla, while Gyurko et al. measured only the height of bone loss on the maxillary molars. We have found that measuring the area of bone loss as described by Tatakis and Guglielmoni (30), with minor modifications, is more accurate than measuring the distance from the alveolar bone crest to the cemento-enamel junction as undertaken by Gyurko et al. (15).

In conclusion, the results of our study indicate that $iNOS$ knockout mice exhibit more extensive soft tissue damage and alveolar bone loss in response to *P. gingivalis* infection, when compared to wild-type mice. The local immune

response to *P. gingivalis* in iNOS knockout mice is characterized by increased PMN numbers in the skin abscess, while the systemic immune response is characterized by high levels of IL-12 in serum. Inducible NOS is required for an appropriate response to *P. gingivalis* infection.

Acknowledgments

We would like to thank Dr Phil Bird for providing the bacteria. Permission to breed the iNOS mice was granted by Prof. Carl Nathan, Cornell University Medical College, USA. This work was funded by the Australian Dental Research Foundation.

References

- Baker PJ, Dixon M, Evans RT, Dufour L, Johnson E, Roopenian DC. CD4(+) T cells and the proinflammatory cytokines gamma interferon and interleukin-6 contribute to alveolar bone loss in mice. *Infect Immun* 1999; **67**: 2804–2809.
- Batista A, Silva T, Chun J, Lara V. Nitric oxide synthesis and severity of human periodontal disease. *Oral Dis* 2002; **8**: 254–260.
- Bird PS, Gemmell E, Polak B, Paton RG, Sosroseno W, Seymour GJ. Protective immunity to *Porphyromonas gingivalis* infection in a murine model. *J Periodontol* 1995; **66**: 351–362.
- Blix I, Helgland K. LPS from *Actinobacillus actinomycetemcomitans* and production of nitric oxide in murine macrophages. *Eur J Oral Sci* 1998; **106**: 576–581.
- Bogdan C. Nitric oxide and the immune response. *Nature* 2001; **2**: 907–916.
- Brandi M, Hukkanen M, Umeda T et al. Bidirectional regulation of osteoclast function by nitric oxide synthase isoforms. *Proc Natl Acad Sci U S A* 1995; **92**: 2954–2958.
- Buttery L, Aguirre IJ, Hukkanen M et al. Nitric oxide stimulates osteoblast replication and development. *J Bone Miner Res* 1999; **14**: 1154.
- Chae H, Park R, Chung H et al. Nitric oxide is a regulator of bone remodelling. *J Pharm Pharmacol* 1997; **49**: 897–902.
- Chiang T, Woo-Rasberry V, Cole F. Role of platelet endothelial form of nitric oxide synthase in collagen–platelet interaction: regulation by phosphorylation. *Biochim Biophys Acta* 2002; **1592**: 169–174.
- Cohen DW, Morris AL. Periodontal manifestation of cyclic neutropenia. *J Periodontol* 1961; **32**: 159–168.
- Dennison DK, Van Dyke TE. The acute inflammatory response and the role of phagocytic cells in periodontal health and disease. *Periodontol 2000* 1997; **14**: 54–78.
- Gemmell E, Kjeldsen M, Yamazaki K, Nakajima T, Aldred M, Seymour GJ. Cytokine profiles of *Porphyromonas gingivalis*-reactive T-lymphocyte line and clones derived from *P. gingivalis*-infected subjects. *Oral Dis* 1995; **1**: 139–146.
- Gemmell E, Winning T, Bird PS, Seymour GJ. Cytokine profiles of lesional and splenic T-cells in *Porphyromonas gingivalis* infection in a murine model. *J Periodontol* 1998; **69**: 1131–1138.
- Gyurko R, Boustany G, Huang PL et al. Mice lacking inducible nitric oxide synthase demonstrated impaired killing of *Porphyromonas gingivalis*. *Infect Immun* 2003; **71**: 4917–4924.
- Gyurko R, Shoji H, Battaglino R et al. Inducible nitric oxide synthase mediates bone development and *P. gingivalis*-induced alveolar bone loss. *Bone* 2005; **36**: 472–479.
- Hamilton RE, Giansanti JS. The Chediak–Higashi syndrome. Report of a case and review of the literature. *Oral Surg Oral Med Oral Pathol* 1974; **37**: 754–761.
- Huang FP, Niedbala W, Wei XQ et al. Nitric oxide regulates Th1 cell development through the inhibition of IL-12 synthesis by macrophages. *Eur J Immunol* 1998; **28**: 4062–4070.
- Kendall H, Haase HR, Li H, Xia Y, Bartold PM. Nitric oxide synthase type-2 is synthesized by human gingival tissue and cultured human gingival fibroblasts. *J Periodontol Res* 2000; **35**: 194–200.
- Laurent M, Lepoivre M, Tenu J. Kinetic modelling of the nitric oxide gradient generated *in vitro* by adherent cells expressing inducible nitric oxide synthase. *Biochem J* 1996; **314**: 109–113.
- MacIntyre I, Zaidi M, Alam A et al. Osteoclastic inhibition: an action of nitric oxide not mediated by cyclic GMP. *Proc Natl Acad Sci U S A* 1991; **88**: 2936–2940.
- MacMicking JD, Nathan C, Hom G et al. Altered responses to bacterial infection and endotoxic shock in mice lacking inducible nitric oxide synthase. *Cell* 1995; **81**: 641–650.
- McLean A, Wei XQ, Huang FP, Al-Alem UAH, Chan WL, Liew FY. Mice lacking inducible nitric oxide synthase are now more susceptible to herpes simplex virus infection despite enhanced Th1 cell responses. *J Gen Virol* 1998; **79**: 825–830.
- Moncada S, Higgs E. Endogenous nitric oxide: physiology, pathology and clinical relevance. *Eur J Clin Invest* 1991; **21**: 361–374.
- Ralston S, Ho L, Helfrich M, Grabowski P, Johnston P, Benjamin N. Nitric oxide: a cytokine induced regulator of bone resorption. *J Bone Miner Res* 1995; **10**: 1040–1049.
- Ralston S, Todd D, Helfrich M, Benjamin N, Grabowski P. Human osteoblast-like cells produce nitric oxide and express inducible nitric oxide synthase. *Endocrinology* 1994; **135**: 330–336.
- Riancho J, Salas E, Zarrabeitia M et al. Expression and functional role of nitric oxide synthase in osteoblast-like cells. *J Bone Miner Res* 1995; **10**: 439–446.
- Schletter J, Heine H, Ulmer A, Rietschel E. Molecular mechanisms of endotoxin activity. *Arch Microbiol* 1995; **164**: 383–389.
- Socransky SS, Haffajee AD. The bacterial aetiology of destructive periodontal disease: current concepts. *J Periodontol* 1992; **63**: 322–331.
- Springer TA, Thompson WS, Miller LJ, Schmalstieg FC, Anderson D. Inherited deficiency of the Mac-1, LFA-1, p150,95 glycoprotein family and its molecular basis. *J Exp Med* 1984; **160**: 1901–1918.
- Tatakis DN, Guglielmoni P. HLA-B27 transgenic rats are susceptible to accelerated alveolar bone loss. *J Periodontol* 2000; **71**: 1395–1400.
- Taylor EL, Megson IL, Haslett C, Rossi AG. Dissociation of DNA fragmentation from other hallmarks of apoptosis in nitric oxide-treated neutrophils: differences between individual nitric oxide donor drugs. *Biochem Biophys Res Commun* 2001; **289**: 1229–1236.
- van't Hof R, Ralston S. Cytokine-induced nitric oxide inhibits bone resorption by inducing apoptosis of osteoclast progenitors and suppressing osteoclast activity. *J Bone Miner Res* 1997; **12**: 1797–1804.
- van't Hof R, Ralston S. Nitric oxide and bone. *Immunology* 2001; **103**: 255–261.
- Wei XQ, Charles IG, Smith A. Altered immune responses in mice lacking inducible nitric oxide synthase. *Nature* 1995; **375**: 408–411.
- Xie QW, Cho J, Calaycay RA et al. Cloning and characterization of inducible nitric oxide synthase from mouse macrophages. *Science* 1992; **256**: 225–228.

This document is a scanned copy of a printed document. No warranty is given about the accuracy of the copy. Users should refer to the original published version of the material.